Full length article

Bioprinting of stem cell expansion lattices ☆

Christopher D. Lindsay [a], Julien G. Roth [b], Bauer L. LeSavage [c], Sarah C. Heilshorn [a],*

[a] Department of Materials Science and Engineering, Stanford University, 496 Lomita Mall, Stanford, CA 94305, USA
[b] Institute for Stem Cell Biology and Regenerative Medicine, Stanford Medical School, Stanford University, 265 Campus Drive, 3rd Floor, Stanford, CA 94305, USA
[c] Department of Bioengineering, Stanford University, 443 Via Ortega, Shriram Center, Room 119, Stanford, CA 94305, USA

ARTICLE INFO

ABSTRACT

Stem cells have great potential in regenerative medicine, with neural progenitor cells (NPCs) being developed as a therapy for many central nervous system diseases and injuries. However, one limitation to the clinical translation of stem cells is the resource-intensive, two-dimensional culture protocols required for biomanufacturing a clinically-relevant number of cells. This challenge can be overcome in an easy-to-produce and cost-effective 3D platform by bioprinting NPCs in a layered lattice structure. Here we demonstrate that alginate biopolymers are an ideal bioink for expansion lattices and do not require chemical modifications for effective NPC expansion. Alginate bioinks that are lightly crosslinked prior to printing can shield printed NPCs from potential mechanical damage caused by printing. NPCs within alginate expansion lattices remain in a stem-like state while undergoing a 2.5-fold expansion. Importantly, we demonstrate the ability to efficiently remove NPCs from printed lattices for future down-stream use as a cell-based therapy. These results demonstrate that 3D bioprinting of alginate expansion lattices is a viable and economical platform for NPC expansion that could be translated to clinical applications.

© 2019 Published by Elsevier Ltd on behalf of Acta Materialia Inc.

1. Introduction

Stem cell-based therapies have shown great potential to benefit patients across a wide range of medical conditions [1]. Stem cells are multipotent cells that have the capacity to regenerate tissue both through differentiation into specific cell lineages and through secretion of regenerative factors [2,3]. While stem cells have shown promise in regenerative medicine, there are still significant hurdles that must be overcome. One such challenge is the large number of cells required to treat a single patient [4–6]. To meet this need, three-dimensional (3D) expansion platforms have emerged as an efficient method to manufacture clinically-relevant numbers of stem cells in a significantly smaller footprint than traditional two-dimensional (2D) culture [7]. Because different types of stem cells have different culture requirements [2,8], the effective and affordable biomanufacturing of distinct stem cell types may require the design and validation of unique expansion strategies.

Towards this goal, we have recently identified matrix remodeling as a requirement for the 3D expansion of adult murine neural progenitor cells (NPCs) [8]. NPCs are multipotent stem cells found in the central nervous system (CNS) that are capable of proliferation and differentiation into the most common lineages present in the CNS [9]. Transplanted NPCs have been identified as a potential therapy for a number of CNS dysfunctions including spinal cord injury, stroke, and amyotrophic lateral sclerosis (ALS), with several clinical trials underway [10,11]. Recent reports have indicated that clinical-grade NPCs (i.e. those expanded using Current Good Manufacturing Practices) may not have the same regenerative efficacy as research-grade NPCs used in pre-clinical models, which limits their value as a translational therapy without further improvement of NPC expansion protocols [12,13]. Achieving clinically relevant numbers of high-quality NPCs using 3D expansion culture will require the development of new biomanufacturing platforms.

Manufacturing NPCs in 3D reduces the spatial footprint of expansion when compared to traditional, adherent 2D culture, thereby reducing the energy and reagent costs, increasing the space-efficiency, and potentially improving the ease of handling. NPCs have been expanded in 3D either through culture as neurospheres (i.e. non-adherent, multicellular aggregates) [14,15] or through encapsulation within bulk hydrogels [8]. However, both neurospheres and bulk gel systems are limited by the insufficient

---

diffusion of oxygen, nutrients, and waste. In neurosphere culture, the slow rate of transport through the cell-dense aggregate results in apoptosis at the core and inhomogeneous cell populations, especially for spheroids >200 μm [16,17]. In 3D bulk hydrogels, the overall size of the construct is limited, since cells further than 200 μm from a free-surface can suffer from limited diffusion of oxygen and nutrients through the gel [18–20]. To overcome these transport limitations, we propose using a 3D-printed lattice of a cell-laden hydrogel as an efficient NPC expansion platform. Here, 3D-printing enables the rapid creation of large-scale, cell-laden scaffolds with an open lattice structure to eliminate diffusional limitations in an easy-to-handle hydrogel.

An often unexplored aspect of designing effective platforms for 3D stem cell expansion is extraction of expanded cells following culture. Efficient extraction of stem cells from the expansion platform (i.e. high cell viability while maintaining stemness) is required whether the stem cells are to be used directly for therapeutic applications or other biomanufacturing processes. While others have demonstrated expansion of stem cells in 3D [7,21,22], there has been limited characterization of extraction efficiency from scalable expansion platforms. Beyond simply remaining viable, extracted cells must retain their stemness to be clinically relevant; thus, quantitative characterization of cell phenotype after expansion and extraction is a prerequisite for eventual clinical translation.

To fabricate this platform, we first must select an appropriate bioink. An ideal gel-based bioink scaffold for NPC expansion has several requirements. First, the gel must mechanically support the NPCs before and after printing [23–25]. Second, the gel must result in high cell viability throughout the printing and post-printing process. Third, the bioink must be remodelable by NPCs. We recently reported that NPCs cultured as single-cells within a 3D matrix must be able to remodel the scaffold to initiate cell-cell contacts between neighboring NPCs in order to maintain their stemness and effectively proliferate [8]. Finally, the bioink must enable the efficient extraction of NPCs after they have been expanded for down-stream use in cell-therapies or for further differentiation.

Electrostatically crosslinked alginate is a popular bioink material that can be manipulated to have all of the required functionalities for an ideal NPC expansion scaffold [26,27]. Alginate is a polysaccharide biopolymer that can be crosslinked through electrostatic bonding with divalent cations to form hydrogels with tunable mechanical stiffness [28]. Furthermore, because electrostatic bonds are reversible, the crosslinked hydrogels exhibit stress relaxation and can be remodeled by encapsulated cells [8,28]. We hypothesized that alginate bioinks subject to distinct first- and second-stage cation crosslinker concentrations would make capable NPC expansion lattices. First-stage crosslinking with a low cation concentration produces a weak, extrudable gel before printing. This weak gel can prevent cell sedimentation within the ink cartridge and protect the cell membrane from damage during printing. Second-stage crosslinking with a high cation concentration produces a stiffer material post-printing that is remodelable, supports cell-cell contacts, promotes cell proliferation, and permits dissociation for on-demand gel extraction of expanded NPCs. Here, we provide demonstration that 3D-printed, cell-laden alginate lattices are a scalable and effective approach to producing clinically-relevant numbers of NPCs that maintain their multipotent potential.

2. Materials and methods

2.1. Alginate bioink preparation

Two versions of ultrapure sodium alginate were purchased from FMC Biopolymers: LVG (low viscosity, G/M ratio > 1.5) and VLVG

(very low viscosity, G/M ratio > 1.5), with molecular weight ranges of 75–200 kDa and > 75 kDa, respectively. Alginate was dissolved in double deionized (DI) water, sterilized by filtering through a 0.22 μm filter (Millipore), and lyophilized for 48 h. RGD-modified alginate was prepared as previously described by coupling a GGGRGDSP peptide (Genscript) onto LVG alginate using standard carbodiimide chemistry [29]. Peptide content of RGD-modified alginate was determined to be $50 \pm 4\ \mu g\ mg^{-1}$ LVG (n = 3) by bicinchoninic acid assay (BCA, Thermo Fisher Pierce) following the manufacturer's recommended procedure. Alginate solutions were dissolved in Neurobasal-A Medium (Gibco) to working concentrations of 3% (w/v) prior to formation of hydrogels. For the alginate screen (Fig. 1B), the stiffest alginate formulations were 2% LVG alginate, the most compliant were 2% VLVG alginate, and the intermediate stiffness were 1% LVG and 1% VLVG. RGD-modified LVG alginate was blended with the unmodified LVG alginate to create a stiff bioink with 1 mM RGD. Similarly, RGD-modified LVG alginate was blended with the unmodified VLVG alginate to create an intermediate stiffness bioink with 0.7 mM RGD. For bioink formulations with first-stage crosslinking, $CaSO_4$ (Sigma-Aldrich) was added to Dulbecco's phosphate buffered saline (DPBS) and mixed with LVG alginate using two 3-mL (BD Biosciences) syringes and a 90° Luer-lock connector (Cole-Parmer) to yield a 2% alginate and 8 mM Ca^{2+} gel.

2.2. Bioink mechanical characterization

Mechanical testing of alginate bioinks was performed using an ARG2 (TA Instruments) stress-controlled rheometer. Stiffness measurements were performed using an 8 mm parallel plate, a 1.0 mm

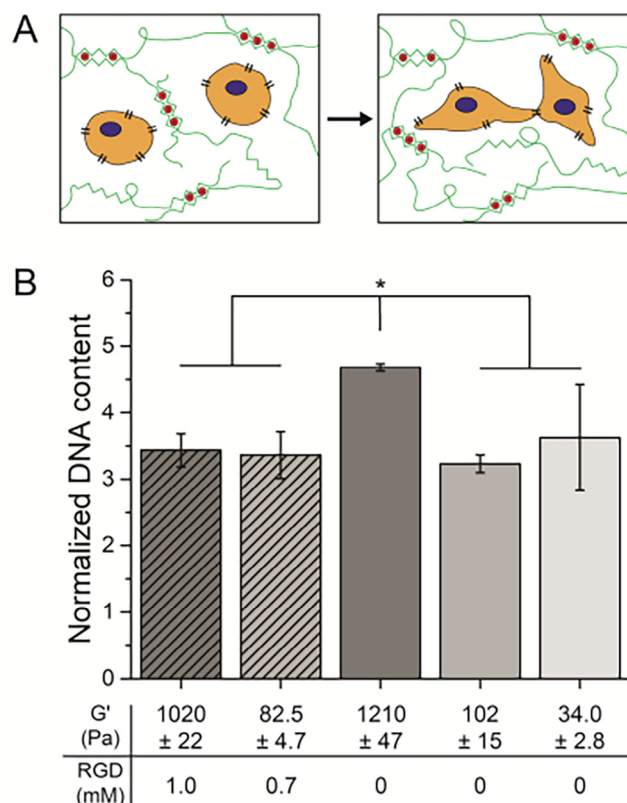|					
G' (Pa)	1020 ± 22	82.5 ± 4.7	1210 ± 47	102 ± 15	34.0 ± 2.8
RGD (mM)	1.0	0.7	0	0	0

Fig. 1. NPCs proliferate over a range of hydrogel stiffnesses and cell-adhesive ligand concentrations. A. Proliferation and stemness maintenance of NPCs in electrostatically crosslinked alginate hydrogels is enabled by matrix remodeling and cell-cell contacts. B. NPC proliferation via total DNA quantification in alginate hydrogels shows little dependence on alginate shear storage modulus, G′, or cell-adhesive ligand (RGD) concentration. All data are normalized to day 0.

gap, and approximately 40 μL of alginate solution extruded through an 18 G needle. For measurements requiring second stage crosslinking, samples were deposited under the parallel plate in a 6-well plate affixed to the rheometer stage, allowed to equilibrate for 10 min, and then 3.75 mL of Neurobasal-A Medium containing 5 or 30 mM $CaCl_2$ was added gently to the well. Four independent trials were performed for each material to ensure reproducibility. Each sample was equilibrated for 3 min for first-stage crosslinking and 1 h for second-stage crosslinking prior to exposure to an amplitude sweep in oscillatory shear at 1 rad s^{-1}. We report the average storage modulus for a representative sample within the linear viscoelastic regime. Shear thinning and modulus recovery experiments were performed using a 20 mm 1° cone and plate geometry with a gap of 28 μm and a sample volume of 45 μL. Shear thinning was assessed by measuring the viscosity under alternating high (10 s^{-1}) and low (0.1 s^{-1}) shear rates performed for 30 s each. For modulus recovery, the oscillatory shear modulus at 1% strain and 1 rad s^{-1} was recorded before and after a shear flow rate of 10 s^{-1} for 1 min.

2.3. Murine neural progenitor cell culture

Adult murine hippocampal NPCs, micro-dissected from the dentate gyrus, were kindly provided by Prof. Theo Palmer (Stanford University) [30]. All protocols were approved by the Stanford Administrative Panel on Laboratory Animal Care, and adhered to the National Institutes of Health (NIH) guidelines for the care and use of laboratory animals (NIH Publication #85-23 Rev. 1985). NPCs were cultured following a previously described protocol [8]. Briefly, NPCs were cultured in Stemness Maintenance Medium (Neurobasal-A, 2% B27 Supplement with Vitamin A (Gibco), GlutaMAX (Gibco), 20 ng ml^{-1} FGF-2 (PeproTech), 20 ng ml^{-1} EGF (PeproTech), and 1% Pen/Strep (Gibco)) on tissue culture plastic coated with 10 μg mL^{-1} polyornithine (Sigma-Aldrich) and 5 μg mL^{-1} laminin (Gibco) at a seeding density of 10,000 NPCs cm^{-2}. Culture medium was replaced every two days. When the NPCs reached approximately 80% confluency, they were dissociated though trypsinization (Gibco), pelleted, resuspended, counted, and either plated back onto coated cell culture surfaces or encapsulated within alginate. NPCs were used between passages 14 and 18.

Murine neural spheroids were formed using AggreWell800 plates (Stemcell Technologies) in accordance with the manufacturer's instructions. Briefly, air bubbles were removed from the AggreWell plate by adding 1 mL per well of Stemness Maintenance Medium and centrifuging at 1300×g for 5 min in a swinging bucket rotor fitted with a plate holder. The media was aspirated, and 1 mL of Stemness Maintenance Media was added to any well receiving cells. A single-cell suspension of murine NPCs was added to each well to create aggregates composed of 10,000 cells per aggregate. The AggreWell plate was then centrifuged at 100×g for 3 min to distribute the cells evenly in the microwells. Daily media changes with Stemness Maintenance Medium were performed for three days in the AggreWell plates at which point the aggregates were manually transferred to individual wells of non-adherent 96 well plates. Daily media changes with Stemness Maintenance Medium continued until Day 14.

2.4. Differentiation of hiPSCs into cortical NPCs

As previously reported [31], human induced pluripotent stem cells (Lines: 8343.2 and 8343.5) were differentiated in N3 media consisting of DMEM/F12 (Thermo Fisher Scientific), Neurobasal (Thermo Fisher Scientific), 1% N-2 Supplement (Thermo Fisher Scientific), 2% B-27 Supplement (Thermo Fisher Scientific), 1% GlutaMax (Thermo Fisher Scientific), 1% MEM NEAA (Thermo Fisher

Scientific), and 2.5 μg mL^{-1} human recombinant insulin (Thermo Fisher Scientific). For the first 11 days, N3 media was further supplemented with 5 μM SB-431542 (Tocris) and 100 nM LDN-193189 (Stemgent). At Day 12, the cells were dissociated with Cell Dissociation Solution (Sigma-Aldrich) and plated onto plates coated with 50 μg mL^{-1} Poly-D-Lysine (Sigma) and 5 μg mL^{-1} Laminin (Roche). hiPSC-derived NPCs were then cultured in N3 media without SB-431542 or LDN-193189 until Day 16 when they were dissociated and encapsulated in alginate. Between Day 1 and Day 16, media changes were performed daily.

2.5. 3D-printing of neural progenitor cells in alginate bioinks

NPCs (final concentration of 30×10^6 NPCs mL^{-1}) were suspended in alginate and mixed with 8 mM CaSO$_4$, as described above, prior to printing. Extrusion was controlled with either a syringe pump (World Precision Instruments) for single-layer scaffolds or a pressure-mediated bioprinter (Allevi) for expansion lattices. Single-layer scaffolds were printed at a rate of 200 μL min^{-1} into cylindrical 4 mm diameter, 0.8 mm thick silicone molds adhered to glass. For 3D bioprinted lattices, custom gcode was written to produce 4-layer scaffolds. All printing was performed at room temperature using a 22 G (Jensen Global) sterile blunt needle affixed to 10 mL plastic syringes (BD Biosciences). Expansion lattices were extruded into a previously described gelatin-based, thermoreversible support bath [32]. Briefly, the support solution was created by dissolving 11.25 g of gelatin (MP Biomedical) in 250 mL of a 10 mM CaCl$_2$ solution. The resultant gelatin solution was allowed to gel in a 500 mL mason jar (Ball) overnight at 4 °C. Following gelation, an additional 250 mL of cold 10 mM CaCl$_2$ solution was added to completely fill the jar. The solution was chilled at −20 °C for 45 min before being blended for 90 sec. The blended gelatin slurry was washed in a 50 mL conical tube (Falcon) with additional cold 10 mM CaCl$_2$ solution and centrifuged at 4500 x g at 4 °C for 3 min. The blended gelatin slurry was washed 4 times, and during the final wash step, 1% Pen/Strep was added to the cold 10 mM CaCl$_2$ solution. For printing, approximately 4 mL of the gelatin slurry was aliquoted into each well of a 6-well plate into which an alginate lattice was to be printed. To homogenize the gelatin and remove any air bubbles, plates with the gelatin slurry were centrifuged at 3200 x g for 3 min. Following printing, the gelatin support slurry was melted at 37 °C for 20 min, aspirated, and replaced with Stemness Maintenance Medium supplemented with CaCl$_2$.

2.6. Quantification of acute cell viability, cell sedimentation, proliferation, and metabolic activity

Acute cell viability following extrusion was characterized by LIVE/DEAD staining (Invitrogen), following the manufacturer's instructions (n = 4). Cell sedimentation was performed as previously described [23]. Briefly, 70 μL of bioink containing NPCs were mixed with 4 μM calcein AM and added to a 70 μL microcuvette (BrandTech) and incubated at 37 °C for 1 h (n = 3). Following incubation, the cuvette was quickly turned on its side and imaged using a confocal microscope. To characterize the degree of cell proliferation, NPC-containing alginate constructs were manually transferred to a lysis buffer of 20 mM Tris HCl (ThermoFisher Scientific), 150 mM NaCl (ThermoFisher Scientific), 0.5% Triton X-100 (Sigma-Aldrich), in DPBS, pH 7.4, and disrupted by sonication. Total DNA content was quantified with the Quant-iT PicoGreen dsDNA Assay Kit (Invitrogen) (n = 4), following the manufacturer's instructions, and normalized to day 0 controls that were collected 30 min post-printing. Metabolic activity of expansion lattices was quantified using CellTiter Blue (Promega), following the manufacturer's instructions (n = 4). Metabolic activity was quantified daily

for 30 min and normalized to the day 1 results. Immediately following quantification, expansion lattices were rinsed in warm Neurobasal-A Medium and Stemness Maintenance Medium was added.

2.7. Characterization of stemness maintenance and mixed differentiation

Stemness maintenance and differentiation capacity were characterized with quantitative reverse transcription polymerase chain reaction (RT-qPCR) as well as immunocytochemistry. Samples destined for analysis with RT-qPCR were transferred to TRIzol reagent (Invitrogen), stored at $-80\,°C$, and disrupted by sonication. RNA was isolated using Phase Lock gels (5 Prime) and reverse transcribed with the High-Capacity cDNA Reverse Transcription Kit (Applied Biosystems). For each well of the 96-Well Reaction Plates (Applied Biosystems), 1320 ng of cDNA from a given sample was diluted in 6.6 µL of nuclease free water and mixed with 8.4 µL of Fast SYBR Green Master Mix (Applied Biosystems). At least four technical replicates (n = 4) were included per sample. Samples were analyzed using an Applied Biosystems StepOnePlus Real Time PCR System. Primers were as follows: Nestin (Fwd: CCCTGAAGTCGAG-GAGCTG; Rev: CTGCTGCACCTCTAAGCGA), Sox2 (Fwd: GCGGAGTG-GAAACTTTTGTCC; Rev: CGGGAAGCGTGTACTTATCCTT), β-tubulin III (Fwd: TAGACCCCAGCGGCAACTAT; Rev: GTTCCAGGTTCCAAGTC-CACC), GFAP (Fwd: CGGAGACGCATCACCTCTG; Rev: AGGGAGTG-GAGGAGTCATTCG). RT-qPCR results are shown as mean ± 95% confidence interval. For immunocytochemistry, gel and 2D samples were fixed with 4% paraformaldehyde in Hanks's buffered salt solution (HBSS, Gibco) at 37 °C for 30 min. Samples were then permeabilized with HBSST (a solution of HBSS, 0.25% Triton X-100, and 30 mM CaCl2) for one hour at room temperature. They were blocked in 5% bovine serum albumin (BSA, Roche) and 5% goat or donkey serum (GS or DS, Gibco) in HBSST for 3 h at room temperature. Primary antibodies were dissolved in HBSS with 2.5% BSA, 2.5% GS or DS, 0.5% Triton X-100, and 30 mM $CaCl_2$ overnight at 4 °C. Primary antibodies were as follows: Nestin (Mouse, BD Pharmingen, 556309, 1:400), Sox2 (Rabbit, Millipore, AB5603, 1:400), β-tubulin III (Mouse, Biolegend, 801202, 1:400), GFAP (Rabbit, Invitrogen, PA1-06702, 1:200), Ki67 (Mouse, Cell Signaling, 9449, 1:400), Pax6 (Rabbit, Biolegend, 901301, 1:200), PhH3 (Goat, Santa Cruz, SC-12927, 1:200). Following four 30 min washes in HBSST, samples were incubated with the following secondary antibodies: AF488 goat anti-rabbit (Invitrogen, A11034, 1:500), AF546 goat anti-mouse (Invitrogen, A11003, 1:500), AF488 donkey anti-rabbit (Invitrogen, A21206, 1:500), or AF647 donkey anti-goat (Invitrogen, A-21447, 1:500) overnight at 4 °C. 4′,6-diamidino-2-phenylindole dihydrochloride (DAPI, Molecular Probes, 1:1000) or phalloidin (Sigma Aldrich, 1:100) were diluted in HBSST and incubated with the samples for one hour at room temperature. Finally, samples were washed in HBSST and mounted with an antifade reagent (Cell Signaling Technologies). All samples were imaged on a Leica SPE confocal microscope.

2.8. Extraction of neural progenitor cells

Encapsulated NPCs were extracted from alginate constructs by first incubating in Stemness Maintenance Medium with 10 µM ROCK Inhibitor (Y-27632, Sigma-Aldrich) for 24 hrs. Constructs were then incubated for 3 min at 37 °C in 200 mM sodium citrate (Sigma-Aldrich) in DPS with 30 mM Glucose (ThermoFischer Scientific) and 10 µM ROCK Inhibitor. The resultant solution was agitated gently with a P1000 pipette and centrifuged at $700\times g$ for 2 min. Following aspiration, the cells were resuspended in Stemness Maintenance Medium or Mixed Differentiation Medium, and plated on polyornithine and laminin coated plates.

2.9. Mixed differentiation of extracted neural progenitor cells

NPCs were cultured with Mixed Differentiation Medium which contained Neurobasal-A, 2% B27 Supplement with Vitamin A, GlutaMAX, 1% fetal bovine serum (FBS) (Sigma-Aldrich), 1 µM retinoic acid (Sigma-Aldrich), and 1% Pen/Strep [33]. Culture medium was replaced every two days. After 7 days in culture, cells were either fixed and stained or collected and lysed.

2.10. Statistical analysis

Calculated data points are reported as mean ± standard deviation, unless otherwise specified. Statistical comparisons between only two groups were made using two-tailed Student's t-test. For comparisons between more than two groups, multiple comparisons tests were used with Tukey *post-hoc* correction. P-values < 0.05 were considered statistically significant. All statistical analyses were performed using OriginPro (OriginLab, 2016).

3. Results

3.1. Alginate hydrogels with a range of mechanics and ligand concentrations support NPC expansion

To efficiently expand NPCs, a material must be remodelable to allow for cell-cell contacts between neighboring NPCs (Fig. 1A). We previously demonstrated that matrix stiffness does not alter NPC stemness and proliferation in covalently crosslinked protein hydrogels [8]. Similarly, it was shown that the presence of cell-adhesive ligands for cellular engagement was not required for NPC expansion within covalently crosslinked protein hydrogels [8]. Therefore, we sought to determine if those matrix properties could be similarly altered in alginate bioinks without affecting NPC expansion.

Several alginate formulations with distinct mechanical and biochemical properties were screened for NPC proliferation. Each bioink formulation contained 2% w/v alginate biopolymer, with the stiffest gels (plateau storage shear modulus, $G' \sim 1$ kPa) using a large molecular weight alginate, the most compliant using a small molecular weight alginate ($G' \sim 30$ Pa), and an intermediate stiffness using a 1:1 blend of these polymers ($G' \sim 100$ Pa). We then formulated cell-adhesive versions of alginate hydrogels with mechanical properties similar to the stiffest and intermediate gels described above. To achieve this, the high molecular weight alginate was functionalized with a cell-adhesive RGD peptide to promote integrin engagement. This RGD-decorated, high-molecular-weight alginate was blended with unmodified, low-molecular-weight alginate to create a new bioink that matched the mechanics of the intermediate stiffness hydrogel. NPCs were expanded over a 7-day culture time within each bioink candidate to test their expansion efficacy without the confounding variable of printing. Proliferation was quantified using total DNA content. All conditions supported NPC expansion and there was little variation across the electrostatically crosslinked alginate bioink conditions (Fig. 1B), which corroborates our previous results for NPC expansion within covalently crosslinked protein hydrogels. Interestingly, the stiffest hydrogel without RGD ligands produced a small yet statistically significant increase in proliferation over the course of the 7-day culture. Thus, the large molecular weight alginate was used for all further experiments.

3.2. Alginate-gel bioinks protect NPCs during printing

The alginate selected for all further printing experiments contained no added cell-adhesive RGD ligands mixed with 8 mM

Ca^{2+}, and 30×10^6 NPCs/mL to create a printable bioink. The addition of calcium to the alginate results in light, first-stage crosslinking to produce a weak gel bioink (Fig. 2A). NPC expansion lattices were then printed into a gelatin slurry with additional calcium cations, 10 mM Ca^{2+}, to stabilize the structure while it was being printed through the introduction of additional second-stage crosslinks. The printed expansion lattices were incubated at 37 °C to melt the gelatin, and the lattices were cultured in calcium-supplemented medium (5 mM Ca^{2+} final concentration) to finalize the second-stage crosslinking. The lightly crosslinked bioink in the print cartridge had a storage modulus, G′, of ∼40 Pa. The printed bioink experienced a 40-fold change in modulus after second-stage crosslinking, with a final modulus of ∼1700 Pa following release from the print bath (Fig. 2B). Light, first-stage crosslinking

of the alginate bioink created a shear thinning and rapidly self-healing material that is compatible with biomanufacturing using an extrusion-based 3D bioprinter. To test the shear-thinning properties of the bioink, alternating high and low shear stress was applied with a rheometer to the first-stage crosslinked bioink (Fig. 2C). The viscosity was greatly reduced under high shear conditions (∼5 Pa·s), demonstrating the bioink's ability to shear-thin and flow. Upon return to a low shear stress, the hydrogel self-healed within 2 s to regain its original viscosity (∼50 Pa·s). The plateau storage and loss moduli were similar before and after application of shear flow at 10 s^{-1} for 1 min (Fig. 2D).

We next evaluated the ability of the bioink to prevent cell sedimentation within the ink cartridge. Cell sedimentation was quantified using the cell sedimentation coefficient, δ, a measure of the
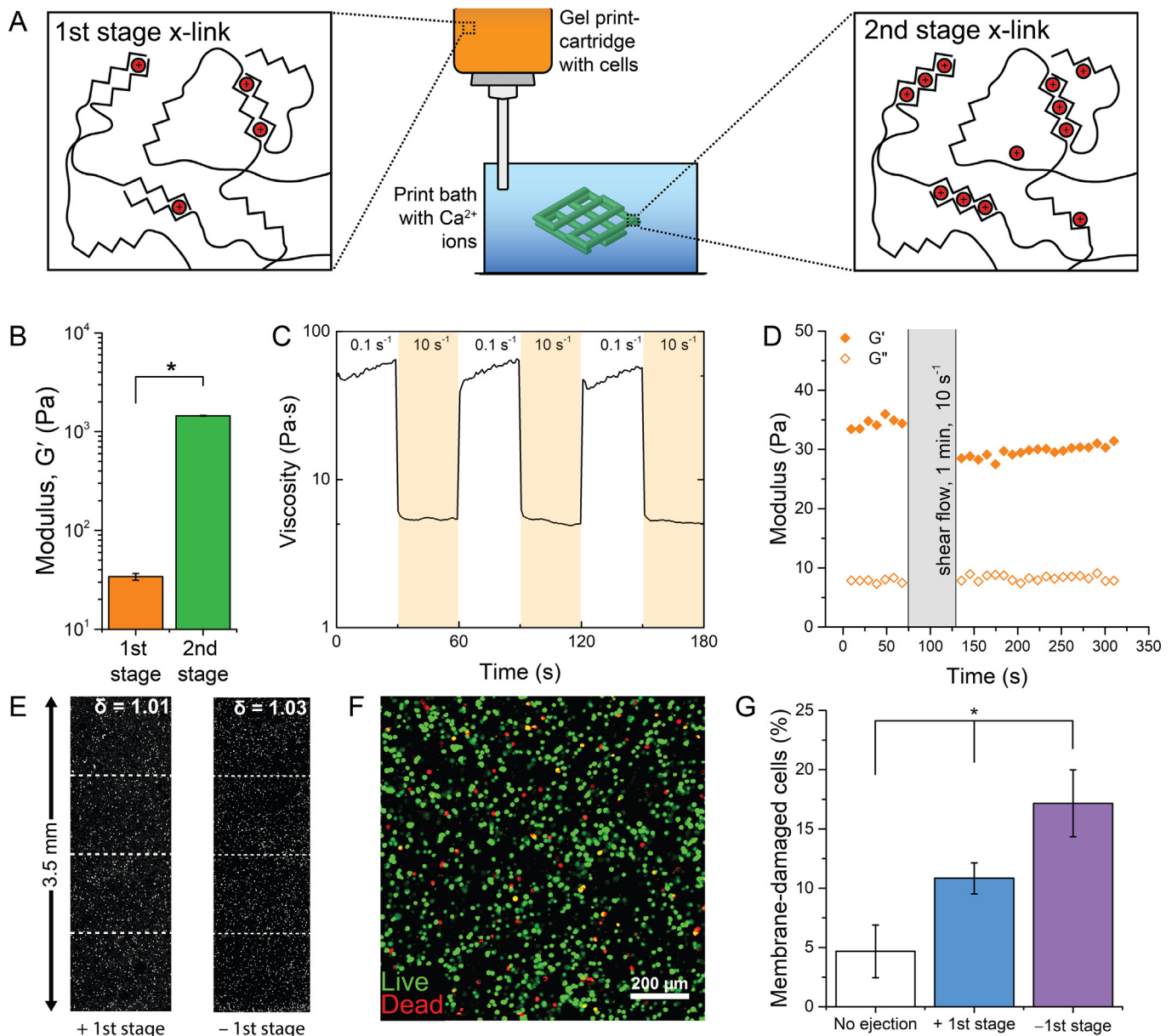

Fig. 2. Alginate hydrogels employing two-stage crosslinking are effective self-healing and cell-protective bioinks for creating alginate expansion lattices. A. Effective bioinks are created using two-stage crosslinked alginate. First-stage crosslinks produce a weak gel that prevents NPC sedimentation and protects cells from mechanical damage during printing. Second-stage crosslinks determine the final bioink modulus. B. First-stage crosslinking produces a low shear storage modulus that increases 40-fold following second-stage crosslinking. C. First-stage crosslinked alginate bioinks shear-thin upon application of high shear rates and quickly recover after removal of high shear rates. D. Alginate bioinks self-heal and quickly recover their mechanical properties after a disruptive shear event. E. No significant cell sedimentation was observed in alginate bioinks after 1 h. With first-stage (+1st) crosslinking: δ = 1.01 ± 0.01, without first-stage (−1st) crosslinking: δ = 1.03 ± 0.03. F, G. Live/Dead is used to quantify membrane damage following print extrusion. First-stage crosslinked alginate bioinks better protect NPCs during extrusion compared to alginate without first-stage crosslinks.

heterogeneity of cell densities across 4 user-defined, vertical zones in each sample, with $\delta = 1$ being homogenously distributed cells [23]. After 1 h, negligible cell sedimentation was observed in the alginate bioink regardless of the presence or absence of first-stage crosslinking (Fig. 2E). During extrusion printing, cells are exposed to mechanical forces that can cause cell membrane damage [34], and some gel-phase bioinks are able to provide mechanical shielding to limit this cell damage [23]. Thus, we quantified cell membrane integrity during bioink printing using a standard Live/Dead assay (Fig. 2F). Upon exposure to printing at 200 μL/min, 10% of NPCs suffered membrane damage in the alginate bioink with first-stage crosslinking. Without first-stage crosslinking, a significantly greater fraction of NPCs, 17%, were damaged. For comparison, only 5% of NPCs not exposed to ejection had damaged membranes.

3.3. NPCs expand in printed alginate lattices

After the alginate molecular weight and concentration of first-stage Ca^{2+} crosslinking was determined, we evaluated the appropriate amount of second-stage Ca^{2+} crosslinking required for efficient NPC expansion. Alginate bioinks (8 mM Ca^{2+}, 30 x10^6 NPCs/mL, 2% w/v) were extruded through a 22-gauge needle to form a single layer within a 4 mm diameter silicone mold. NPC Stemness Maintenance Medium supplemented with either 5 mM or 30 mM Ca^{2+} was added to completely submerge the culture. The plateau storage modulus of the gels in 5 mM and 30 mM Ca^{2+} supplemented media were 1449 ± 11 Pa and 18,850 ± 80 Pa, respectively. Both media conditions produced scaffolds that were easy to handle and did not appear to erode during a 7-day culture. To quantify NPC proliferation within the bioinks, total DNA content was assessed. NPCs cultured in the 5 mM Ca^{2+} medium expanded 2-fold after 3 days in culture and 2.5-fold after 7 days, and showed significantly higher proliferation when compared to NPCs expanded in the 30 mM condition (Fig. 3A). Thus, 5 mM Ca^{2+} supplementation was used to print a multilayer expansion lattice within a gelatin slurry support bath. The expansion lattices were produced by extruding alternating "S"-shaped layers at a 90° angle to the layer immediately below (Fig. 3B). Lattices measured 10 mm on a side and were comprised of 4 layers. The bioink was printed through a 22-gauge needle (radius: 206 μm) resulting in a filament size estimated to be approximately 400 μm in diameter. Each layer used approximately 11 μL of NPC bioink and contained 330,000 NPCs. Following extrusion, the printed NPC expansion lattices and gelatin slurry were incubated for 20 min at 37 °C to release

the lattice from the gelatin (Fig. 3A). The expansion lattices were washed and placed in NPC expansion medium with supplemented Ca^{2+} at 5 mM to finalize the bioink second-stage crosslinking. The printed expansion lattices were assessed daily for metabolic activity as a non-destructive indicator of cell number. Metabolic activity increased two-fold after two days in culture and then maintained this plateau value for one week (Fig. 3C).

3.4. NPCs expanded in alginate bioinks maintain their stem-like phenotype

Functional stem cells have the capacity to self-renew while maintaining their stem-like phenotype. NPCs specifically require the ability to remodel their surrounding matrix and establish cell-cell contacts to maintain their stemness in 3D matrices [8]. To characterize their stemness, NPCs were cultured in printed, single-layer, alginate bioinks and 5 mM Ca^{2+} supplemented medium for up to 1 week and observed using immunocytochemistry (ICC). Actin cytoskeletal staining of the NPCs in the bioinks revealed spheroid-like clusters, approximately 20 μm in diameter (Fig. 4A). NPC cell clusters were well distributed throughout the printed construct and did not appear connected. Proliferation and stemness maintenance in the NPC clusters was observed by staining for Ki-67, Sox2, and nestin. Ki-67 is a nuclear protein that is found only in cells that are active in the cell-cycle and are proliferating. The transcription factor Sox2 and the intermediate filament protein nestin are markers for stemness-maintenance in NPCs [35]. All of the stained nuclei in NPC clusters cultured for 3 days in 5 mM Ca^{2+} supplemented medium were positive for Sox2, while only a subset were positive for Ki-67 (Fig. 4B), signifying that some, but not all, NPCs were actively proliferating at the time of collection. All observed NPC cell clusters within the printed lattices were positive for both nestin and Sox2 (Fig. 4C). To demonstrate the potential use of this technology to expand a clinically relevant cell type, we encapsulated human induced pluripotent stem cell-derived NPCs (hiPSC-NPCs) within this same alginate biomaterial. Similar to murine NPCs, these 3D cultures of hiPSC-NPCs expanded to form cell clusters with positive staining for stemness and proliferation markers (Fig. S1).

To corroborate the phenotypic stemness maintenance results provided by ICC, mRNA expression of nestin and Sox2 were assessed over 7 days in culture in both 5 mM and 30 mM Ca^{2+} supplemented media. NPCs cultured in the 5 mM Ca^{2+} condition for 3 days show no change in their nestin and Sox2 levels, while NPCs cultured in the 30 mM Ca^{2+} condition show a significant decrease
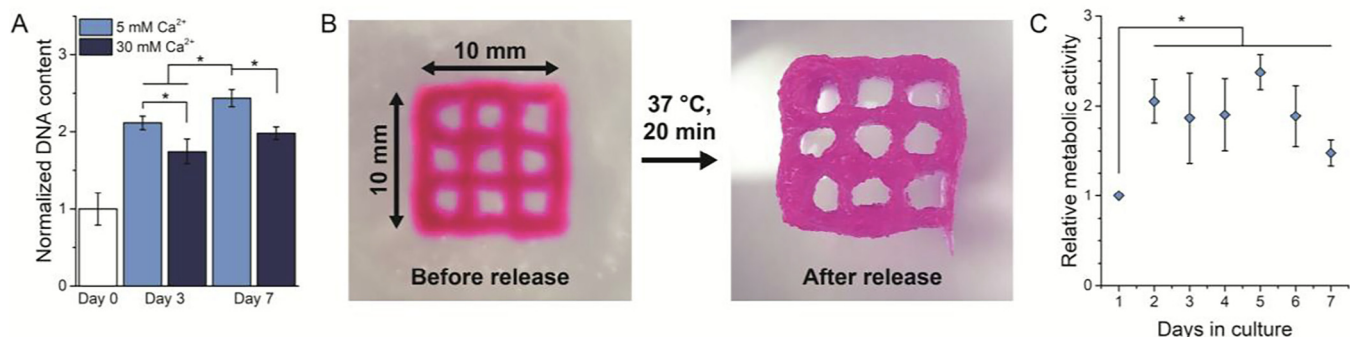

Fig. 3. Printed expansion lattices support proliferation for 1 week. A. Total DNA quantification of cells in single-layer alginate scaffolds indicates a significant increase in cell number over the course of 1 week for bioinks in both low and high concentrations of calcium-supplemented media, 5 mM and 30 mM Ca^{2+}, respectively. NPCs in scaffolds cultured in low calcium-supplemented medium proliferate more than those cultured in high calcium-supplemented medium. All data are normalized to day 0. B. Expansion lattices are printed into a gelatin slurry and contain 4 connected, "S"-shaped layers. Heating is used to release lattices from the slurry, and lattices are cultured in calcium-supplemented medium. C. Total metabolic activity of NPCs in expansion lattices increases after 2 days in culture and remains elevated over 1 week (culture medium included 5 mM Ca^{2+}).
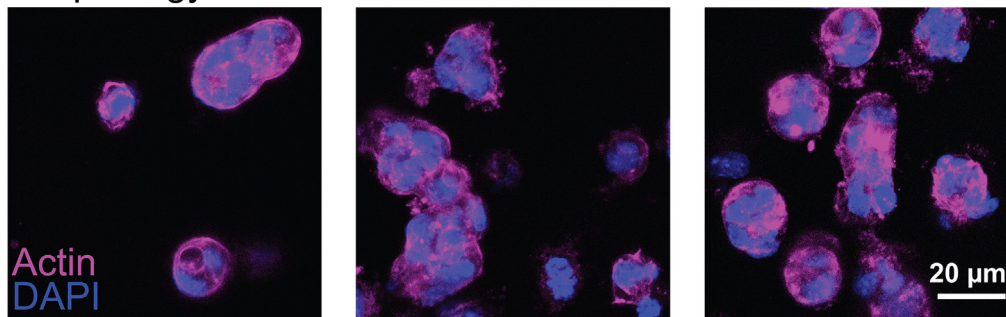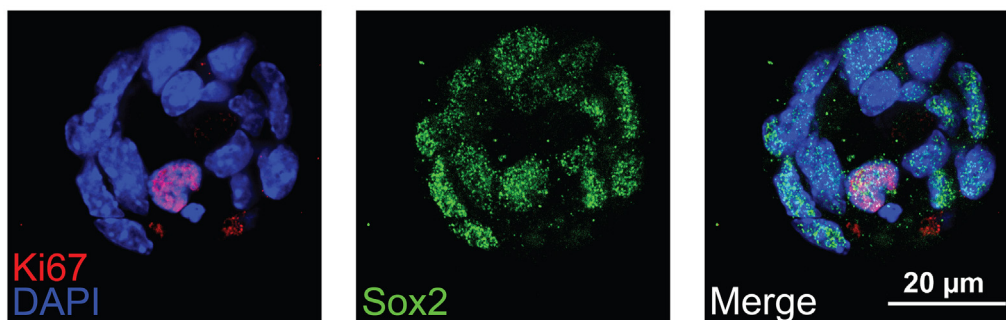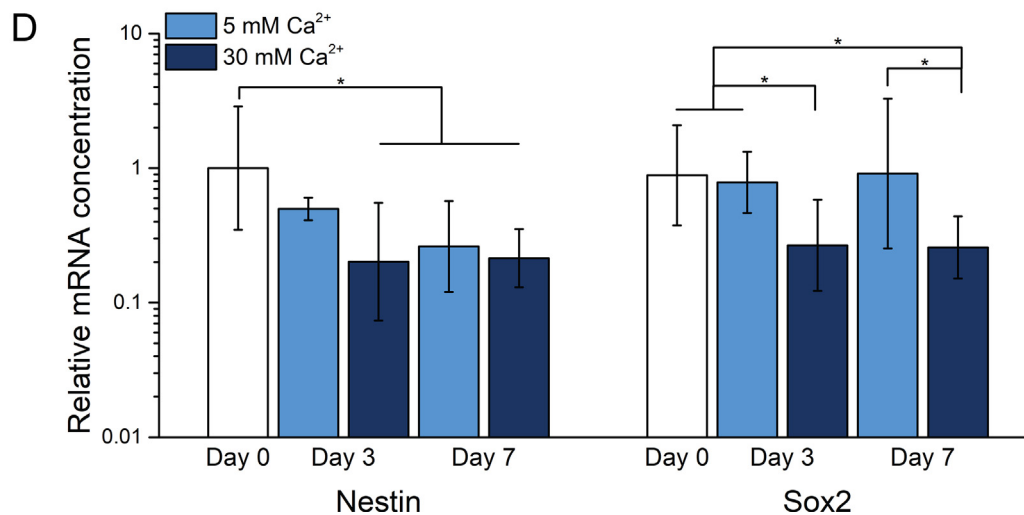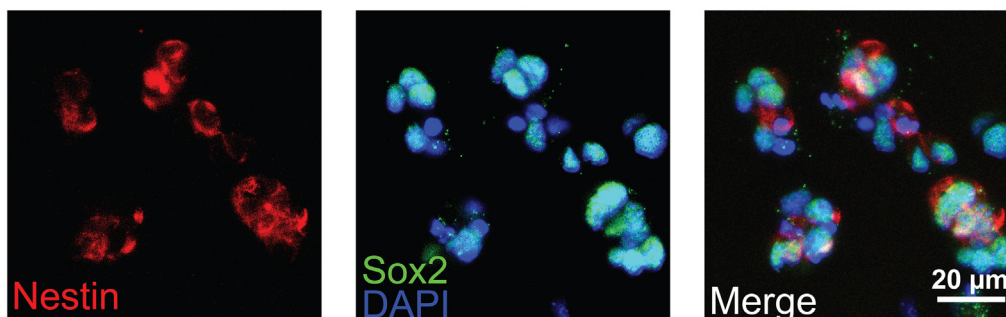
Fig. 4. NPCs grown within expansion lattices maintain stemness. A. Actin cytoskeletal staining of NPCs cultured for 3 days in expansion lattices reveals distributed cell clusters, $\sim 20\ \mu m$ in diameter. B. Colocalization of proliferation marker Ki67 and stemness marker Sox2 in NPC nuclei demonstrates the self-renewal capacity of NPCs grown in expansion lattices. C. NPC cell clusters maintain their stemness as demonstrated by positive staining for nestin and Sox2. D. mRNA expression levels for neural stemness markers nestin and Sox2 are unchanged after 3 days for NPCs in expansion lattices cultured in low calcium (5 mM) supplemented medium. Stemness marker expression is decreased in high calcium (30 mM) supplemented medium.

(Fig. 4D). When cultured for 7 days in the bioink, NPCs in the 5 mM Ca^{2+} condition better retain expression of stemness markers when compared to the 30 mM Ca^{2+} condition. To assess spontaneous, off-target differentiation, we quantified glial fibrillary acidic protein (GFAP) expression in these bioinks as well as in traditional neurosphere cultures, which are known to initiate spontaneous differentiation [36]. After 3 days in culture, NPCs cultured in the 5 mM Ca^{2+} condition showed little evidence of differentiation, while NPCs cultured in 30 mM Ca^{2+} or as spheroids showed a significant commitment towards glial lineages (Fig. S2).

3.5. Extracted NPCs are proliferative and differentiate into neuronal and glial lineages

Following proliferation in an expansion lattice, NPCs must be extracted from the alginate bioink for potential clinical use. To achieve this goal, a protocol for alginate lattice dissociation was developed, and the extracted NPCs were collected for further analysis. Cell-laden scaffolds were placed in warm saline with a divalent cation chelator (200 mM sodium citrate) to chelate calcium from the alginate and destabilize the gel, and a ROCK inhibitor (10 μM Y-27632) to improve the survival of the freshly suspended

NPCs (Fig. 5A). After three minutes of incubation, the solution was gently pipetted for 30 s to fully break apart any remaining hydrogel. The NPC and alginate suspension was centrifuged to form a pellet and resuspended in fresh culture medium. Extracted NPCs were highly viable (79% ± 9%), as determined by Live/Dead assay on freshly extracted cells.

After resuspension, extracted NPCs were ready for further analysis to verify their stemness. By definition, stem cells must be able to self-renew and differentiate into downstream lineages. Thus, extracted NPCs were plated in either Stemness Maintenance Medium or Mixed Differentiation Medium to confirm these stem cell criteria. For NPC renewal, extracted cells were plated on 2D coated tissue culture surfaces with Stemness Maintenance Medium, cultured for 3 days, and evaluated for their stemness markers. Nestin and Sox2 are strongly expressed in extracted NPCs after 3 days (Fig. 5B). This exact same extraction protocol was also used to remove viable hiPSC-NPCs from the matrix, and extracted cells continued to show maintenance of stemness and proliferation markers (Fig. S3). Additionally, these extracted hiPSC-NPCs formed neural rosette-like structures, a known morphology of early neural progenitor cells [37]. A comparison of stemness markers between freshly extracted and 3-day post-
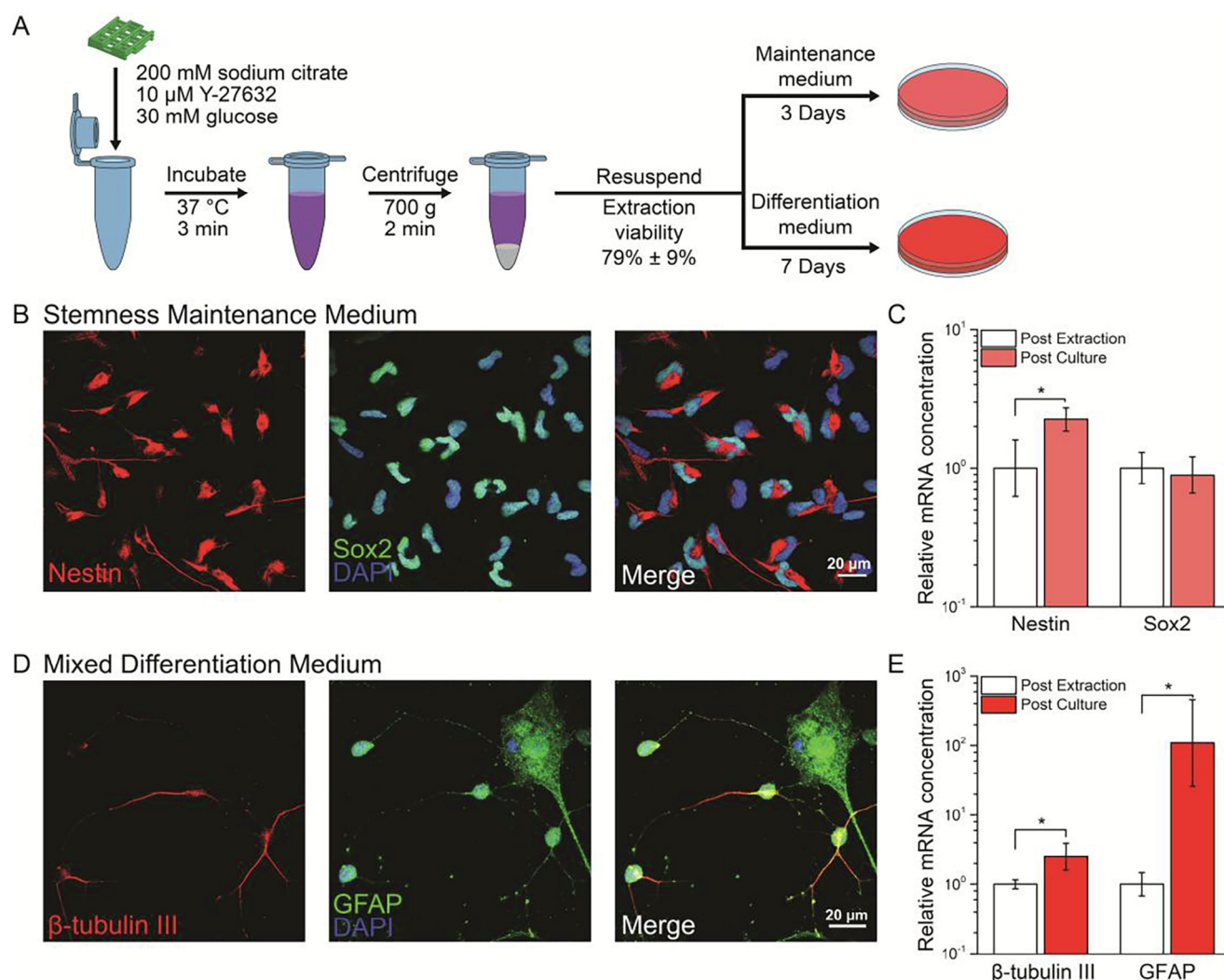

Fig. 5. NPCs extracted from expansion lattices retain their stemness. A. NPCs are extracted from expansion in less than 10 min with high cell viability. Collected NPCs can then be further analyzed for verification of their stemness. B, C. Extracted NPCs cultured for 3 days in Stemness Maintenance Medium retain stemness markers nestin and Sox2 as confirmed by B. immunocytochemistry and C. mRNA expression levels. D, E. Extracted NPCs cultured for 7 days in Mixed Differentiation Medium are able to differentiate down neuronal and glial pathways as confirmed by D. immunocytochemistry, and E. mRNA expression levels of the neuronal marker β-tubulin III and glial marker GFAP.

extraction NPCs using RT-qPCR confirmed a stem-like phenotype in 3-day post-extraction NPCs (Fig. 5C). To confirm their differentiation potential, extracted NPCs were plated on coated tissue culture surfaces and cultured for 7 days in Mixed Differentiation Medium that allowed NPCs to progress along both neuronal and glial lineages. Following culture, neuronal (β-tubulin III) and glial (GFAP) markers were observed in differentiated cells (Fig. 5D). Increased neuronal and glial marker expression in the cells was confirmed using RT-qPCR, with both β-tubulin III and GFAP expression significantly increased after differentiation when compared to freshly extracted NPCs.

4. Discussion

Previously, we reported the use of covalently crosslinked protein hydrogels to identify the key material properties that enable NPC stemness maintenance and proliferation in 3D gels. In this study, we have expanded upon our previous work by evaluating the appropriate alginate bioink properties that can support NPC stemness maintenance and proliferation. We screened multiple alginate bioinks with a range of mechanical and biochemical properties to test their potential effects on NPC proliferation. A significant advantage of the alginate bioinks used here is that they are commercially available and can be used with no chemical modifications. Such a commercially available and unaltered material for NPC expansion should greatly reduce the cost of manufacture and ease bioink translation into clinical applications. Consistent with our previous work using protein hydrogels, our results show that gel stiffness and cell-adhesive ligand concentration do not greatly alter NPC proliferation within an electrostatically crosslinked alginate scaffold (Fig. 1B). Small decreases in proliferation for the more compliant materials when compared to the stiffest materials may be due, in part, to erosion of the weaker alginate scaffolds. We hypothesize that erosion of the more compliant materials resulted in loss of expansion scaffold and, by extension, loss of cells from the scaffold.

Gel-phase bioinks that utilize two stages of crosslinking have distinct advantages over inks that are printed as a viscous solution followed by a single crosslinking step. First-stage crosslinks are beneficial before and during printing, because a gel-phase bioink can prevent cell sedimentation, protect the printed cells from mechanical damage during ejection, and better maintain print fidelity immediately following printing [23]. Alginate is a unique material in that both first- and second-stage crosslinking can be achieved via a single crosslinking mechanism (i.e. electrostatic bonding) (Fig. 2A). Mixing a small amount of calcium with the alginate solution and cells for first-stage crosslinking created a weak, gel-phase bioink that eliminated cell sedimentation and reduced cell damage caused by ejection (Fig. 2E–G). The dynamic first-stage crosslinks quickly reformed after a disruptive shearing force was applied, illustrating that alginate is a robust, self-healing bioink (Fig. 2C, D). Calcium was added to the culture medium following printing to complete the second-stage crosslinking, which stiffened the bioink (Fig. 2B) to provide erosion resistance and durability to the expansion lattices.

Printing expansion lattices within a gelatin slurry enables the creation of complex, freestanding 3D structures that would not be possible in an aqueous or dry environment [32,38]. The gelatin slurry hydrates the sample, preventing lattice dehydration which becomes increasingly important as the size of the scaffold (and hence total printing time) increases. The gelatin slurry was easily washed away after 20 min of incubation at 37 °C, and the expansion lattices could be moved to expansion medium for final crosslinking and incubation (Fig. 3A).

Stemness maintenance of NPCs in 3D gels requires cell-mediated matrix remodeling and subsequent cell-cell contacts, as previously demonstrated in covalently crosslinked protein gels and covalently crosslinked, non-remodelable alginate hydrogels [8]. NPCs in alginate bioinks were able to remodel their environment, forming clusters of proliferative, stem-like cells (Fig. 4A–C). The encapsulated NPCs displayed two traditional neural stemness markers, nestin and Sox2. Importantly, Ki-67, a nuclear marker found in actively proliferating cells, was co-localized with Sox2, confirming that stemness maintenance is associated with active proliferation, as previously demonstrated [8]. NPC proliferation and stemness maintenance was greater in gels with lesser amounts of secondary crosslinking (Fig. 3B). This may be due to an increase in the rate of matrix remodeling in the more lightly crosslinked gel, enabling greater cell-cell contact, and increased stemness maintenance.

To be clinically relevant, expanded NPCs must be efficiently extracted from the 3D expansion lattice. In developing a protocol for cell extraction, there were several challenges that needed to be addressed. The first challenge was to degrade the expansion lattice using only cytocompatible, buffered conditions. Sodium citrate was used to quickly chelate calcium ions from the alginate scaffolds within three minutes, with gentle mixing being used to finalize the process. The second challenge was cell collection after extraction. Centrifugation was found to efficiently separate the extracted NPCs from the chelated alginate solution. The final challenge was ensuring NPC survival through the course of several mechanical and biochemical manipulations. Y-27632, a ROCK inhibitor often used in suspension cultures of progenitor cells, was employed to prevent cell death during extraction [39]. The ease of cell extraction from our alginate-based expansion system using mild conditions is an attractive advantage for further translation of this technology to other sensitive stem cell types.

After NPCs were collected from printed alginate constructs, additional analysis was performed to confirm their stemness, namely their self-renewal and differentiation potential. Extracted NPCs cultured in Stemness Maintenance Medium successfully retained their stemness markers nestin and Sox2 (Fig. 5B, C). Sox2 showed similar expression while any nestin expression lost during gel culture was recovered following extraction and expansion on tissue culture dishes. Following a mixed differentiation study using a culture medium that supported multiple neural cell lineages, both neuronal (β-tubulin III) and glial (GFAP) markers were upregulated (Fig. 5D, E). Importantly, this shows that both neuronal and glial populations can arise from extracted NPCs, and that the NPCs have maintained their multipotency.

Looking forward, expansion lattices may be a solution to reducing the spatial footprint and energy and reagent resources required to produce large numbers of regenerative stem cells. In this study, approximately 1.32×10^6 cells were encapsulated in a single expansion lattice with a 1-cm^2 footprint for expansion. In comparison, a common 2D seeding density for NPCs is 7.5×10^5 NPCs on a 75 cm^2 flask, which was used in this study. By moving the cells from a 2D-plate culture to a 3D-expansion lattice culture, the footprint for expansion is reduced 132-fold. Put another way, every 150 cm^2 flask used for NPC expansion culture could be replaced with a single well of a 48-well plate (1 cm^2). For a relatively small clinical trial where at least 200 million NPCs were required [40], this reduces the footprint for expansion from 20,000 cm^2 for 2D culture down to 150 cm^2 for an expansion lattice. Furthermore, because 3D bioprinting allows for multiplexing, many expansion lattices could be fabricated in parallel for large-scale expansion that may increase lot sizes past those that are possible with current adherent plate technology in biomanufacturing applications. This reduction in surface area will reduce the amount of resources and time required for expansion of a clinically-relevant number of NPCs or other regenerative cell types.

5. Conclusion

The results presented here demonstrate that 3D bioprinting can be used to fabricate expansion lattices that support the proliferation of NPCs. The alginate bioink presented is commercially available, does not require costly modifications, and can be printed into a multi-layer lattice with a relatively small spatial footprint compared to traditional 2D expansion culture methods. Using a dual-stage crosslinking strategy, the mechanical properties of the bioink were selected to prevent cell sedimentation pre-printing, to prevent cell membrane damage during printing, and to form a robust and stable lattice post-printing. NPCs cultured within expansion lattices were found to retain their capacity for self-renewal and proliferation and were efficiently extracted from the scaffolds with no loss in their stemness. Together, these results suggest that 3D bioprinting will facilitate scaled fabrication of expansion lattices and will promote the translation of cell-based clinical applications.

Acknowledgements

Disclosures

The authors declare no conflict of interest.

Appendix A. Supplementary data

Supplementary data to this article can be found online at https://doi.org/10.1016/j.actbio.2019.05.014.

References

[1] A. Trounson, C. McDonald, Stem cell therapies in clinical trials: progress and challenges, Cell Stem Cell 17 (2015) 11–22, https://doi.org/10.1016/j.stem.2015.06.007.

[2] K.G. Chen, B.S. Mallon, R.D.G. McKay, P.G. Robey, Human pluripotent stem cell culture: considerations for maintenance, expansion, and therapeutics, Cell Stem Cell 14 (2014) 13–26, https://doi.org/10.1016/j.stem.2013.12.005.

[3] V. Tabar, L. Studer, Pluripotent stem cells in regenerative medicine: challenges and recent progress, Nat. Rev. Genet. 15 (2014) 82–92, https://doi.org/10.1038/nrg3563.

[4] D.C. Kirouac, P.W. Zandstra, The systematic production of cells for cell therapies, Cell Stem Cell 3 (2008) 369–381, https://doi.org/10.1016/j.stem.2008.09.001.

[5] T.C. Schulz, H.Y. Young, A.D. Agulnick, M.J. Babin, E.E. Baetge, A.G. Bang, A. Bhoumik, I. Cepa, R.M. Cesario, C. Haakmeester, K. Kadoya, J.R. Kelly, J. Kerr, L.A. Martinson, A.B. McLean, M.A. Moorman, J.K. Payne, M. Richardson, K.G. Ross, E. S. Sherrer, X. Song, A.Z. Wilson, E.P. Brandon, C.E. Green, E.J. Kroon, O.G. Kelly, K.A. D'Amour, A.J. Robins, A scalable system for production of functional pancreatic progenitors from human embryonic stem cells, PLoS One 7 (2012), https://doi.org/10.1371/journal.pone.0037004 e37004.

[6] M. Serra, C. Brito, C. Correia, P.M. Alves, Process engineering of human pluripotent stem cells for clinical application, Trends Biotechnol. 30 (2012) 350–359, https://doi.org/10.1016/j.tibtech.2012.03.003.

[7] Y. Lei, D.V. Schaffer, A fully defined and scalable 3D culture system for human pluripotent stem cell expansion and differentiation, Proc. Natl. Acad. Sci. U.S.A. 110 (2013) E5039–E5048, https://doi.org/10.1073/pnas.1309408110.

[8] C.M. Madl, B.L. LeSavage, R.E. Dewi, C.B. Dinh, R.S. Stowers, M. Khariton, K.J. Lampe, D. Nguyen, O. Chaudhuri, A. Enejder, S.C. Heilshorn, Maintenance of neural progenitor cell stemness in 3D hydrogels requires matrix remodelling, Nat. Mater. 16 (2017) 1233–1242, https://doi.org/10.1038/nmat5020.

[9] S. Goldman, Stem and progenitor cell-based therapy of the human central nervous system, Nat. Biotechnol. 23 (2005) 862–871, https://doi.org/10.1038/nbt1119.

[10] K.I. Park, S. Liu, J.D. Flax, S. Nissim, P.E. Stieg, E.Y. Snyder, Transplantation of neural progenitor and stem cells: developmental insights may suggest new therapies for spinal cord and other CNS dysfunction, J Neurotrauma. 16 (1999) 675–687, https://doi.org/10.1089/neu.1999.16.675.

[11] J. Rosati, D. Ferrari, F. Altieri, S. Tardivo, C. Ricciolini, C. Fusilli, C. Zalfa, D.C. Profico, F. Pinos, L. Bernardini, B. Torres, I. Manni, G. Piaggio, E. Binda, M. Copetti, G. Lamorte, T. Mazza, M. Carella, M. Gelati, E.M. Valente, A. Simeone, A. L. Vescovi, Establishment of stable iPS-derived human neural stem cell lines suitable for cell therapies, Cell Death Dis. 9 (2018) 937, https://doi.org/10.1038/s41419-018-0990-2.

[12] A.J. Anderson, K.M. Piltti, M.J. Hooshmand, R.A. Nishi, B.J. Cummings, Preclinical efficacy failure of human CNS-derived stem cells for use in the pathway study of cervical spinal cord injury, Stem Cell Rep. 8 (2017) 249–263, https://doi.org/10.1016/j.stemcr.2016.12.018.

[13] S.E. Marsh, S.T. Yeung, M. Torres, L. Lau, J.L. Davis, E.S. Monuki, W.W. Poon, M. Blurton-Jones, HuCNS-SC human NSCs fail to differentiate form ectopic clusters, and provide no cognitive benefits in a transgenic model of Alzheimer's disease, Stem Cell Rep. 8 (2017) 235–248, https://doi.org/10.1016/j.stemcr.2016.12.019.

[14] A. Bez, E. Corsini, D. Curti, M. Biggiogera, A. Colombo, R.F. Nicosia, S.F. Pagano, E.A. Parati, Neurosphere and neurosphere-forming cells: morphological and ultrastructural characterization, Brain Res. 993 (2003) 18–29, https://doi.org/10.1016/j.brainres.2003.08.061.

[15] A.M. Pasca, S.A. Sloan, L.E. Clarke, Y. Tian, C.D. Makinson, N. Huber, C.H. Kim, J. Y. Park, N.A. O'Rourke, K.D. Nguyen, S.J. Smith, J.R. Huguenard, D.H. Geschwind, B.A. Barres, S.P. Pasca, Functional cortical neurons and astrocytes from human pluripotent stem cells in 3D culture, Nat. Methods 12 (2015) 671–678, https://doi.org/10.1038/nmeth.3415.

[16] J.B. Jensen, M. Parmar, Strengths and limitations of the neurosphere culture system, Mol. Neurobiol. 34 (2006) 153–161, https://doi.org/10.1385/MN:34:3:153.

[17] C.S. Szot, C.F. Buchanan, J.W. Freeman, M.N. Rylander, 3D in vitro bioengineered tumors based on collagen I hydrogels, Biomaterials 32 (2011) 7905–7912, https://doi.org/10.1016/j.biomaterials.2011.07.001.

[18] L.E. Bertassoni, M. Cecconi, V. Manoharan, M. Nikkhah, J. Hjortnaes, A.L. Cristino, G. Barabaschi, D. Demarchi, M.R. Dokmeci, Y. Yang, A. Khademhosseini, Hydrogel bioprinted microchannel networks for vascularization of tissue engineering constructs, Lab Chip. 14 (2014) 2202–2211, https://doi.org/10.1039/c4lc00030g.

[19] J.S. Miller, K.R. Stevens, M.T. Yang, B.M. Baker, D.H.T. Nguyen, D.M. Cohen, E. Toro, A.A. Chen, P.A. Galie, X. Yu, R. Chaturvedi, S.N. Bhatia, C.S. Chen, Rapid casting of patterned vascular networks for perfusable engineered three-dimensional tissues, Nat. Mater. 11 (2012) 768–774, https://doi.org/10.1038/nmat3357.

[20] F.A. Auger, L. Gibot, D. Lacroix, The pivotal role of vascularization in tissue engineering, Annu. Rev. Biomed. Eng. 15 (2013) 177–200, https://doi.org/10.1146/annurev-bioeng-071812-152428.

[21] Q. Gu, E. Tomaskovic-Crook, R. Lozano, Y. Chen, R.M. Kapsa, Q. Zhou, G.G. Wallace, J.M. Crook, Functional 3D neural mini-tissues from printed gel-based bioink and human neural stem cells, Adv. Healthc. Mater. 5 (2016) 1429–1438, https://doi.org/10.1002/adhm.201600095.

[22] Q. Gu, E. Tomaskovic-Crook, G.G. Wallace, J.M. Crook, 3D Bioprinting human induced pluripotent stem cell constructs for in situ cell proliferation and successive multilineage differentiation, Adv. Healthc. Mater. 6 (2017) 1700175, https://doi.org/10.1002/adhm.201700175.

[23] K. Dubbin, A. Tabet, S.C. Heilshorn, Quantitative criteria to benchmark new and existing bio-inks for cell compatibility, Biofabrication 9 (2017), https://doi.org/10.1088/1758-5090/aa869f 044102.

[24] K. Dubbin, Y. Hori, K.K. Lewis, S.C. Heilshorn, Dual-stage crosslinking of a gel-phase bioink improves cell viability and homogeneity for 3D bioprinting, Adv. Healthc. Mater. 5 (2016) 2488–2492, https://doi.org/10.1002/adhm.201600636.

[25] C.B. Highley, C.B. Rodell, J.A. Burdick, Direct 3D printing of shear-thinning hydrogels into self-healing hydrogels, Adv. Mater. 27 (2015) 5075–5079, https://doi.org/10.1002/adma.201501234.

[26] J.A. Rowley, G. Madlambayan, D.J. Mooney, Alginate hydrogels as synthetic extracellular matrix materials, Biomaterials 20 (1999) 45–53, https://doi.org/10.1016/S0142-9612(98)00107-0.

[27] K.Y. Lee, J.A. Rowley, P. Eiselt, E.M. Moy, K.H. Bouhadir, D.J. Mooney, Controlling mechanical and swelling properties of alginate hydrogels independently by cross-linker type and cross-linking density, Macromolecules 33 (2000) 4291–4294, https://doi.org/10.1021/ma9921347.

[28] A. Bauer, L. Gu, B. Kwee, W.A. Li, M. Dellacherie, A.D. Celiz, D.J. Mooney, Hydrogel substrate stress-relaxation regulates the spreading and proliferation of mouse myoblasts, Acta Biomater. 62 (2017) 82–90, https://doi.org/10.1016/j.actbio.2017.08.041.

[29] O. Chaudhuri, L. Gu, D. Klumpers, M. Darnell, S.A. Bencherif, J.C. Weaver, N. Huebsch, H.P. Lee, E. Lippens, G.N. Duda, D.J. Mooney, Hydrogels with tunable stress relaxation regulate stem cell fate and activity, Nat. Mater. 15 (2016) 326–334, https://doi.org/10.1038/nmat4489.

[30] H. Babu, G. Cheung, H. Kettenmann, T.D. Palmer, G. Kempermann, Enriched monolayer precursor cell cultures from micro-dissected adult mouse dentate gyrus yield functional granule cell-like neurons, PLoS One 2 (2007), https://doi.org/10.1371/journal.pone.0000388 e388.

[31] Y. Shi, P. Kirwan, J. Smith, H.P.C. Robinson, F.J. Livesey, Human cerebral cortex development from pluripotent stem cells to functional excitatory synapses, Nat. Neurosci. 15 (2012) 477–486, https://doi.org/10.1038/nn.3041.

[32] T.J. Hinton, Q. Jallerat, R.N. Palchesko, J.H. Park, M.S. Grodzicki, H.-J. Shue, M.H. Ramadan, A.R. Hudson, A.W. Feinberg, Three-dimensional printing of complex biological structures by freeform reversible embedding of suspended hydrogels e1500758, Sci. Adv. 1 (2015), https://doi.org/10.1126/sciadv.1500758.

[33] K. Saha, A.J. Keung, E.F. Irwin, Y. Li, L. Little, D.V. Schaffer, K.E. Healy, Substrate modulus directs neural stem cell behavior, Biophys. J. 95 (2008) 4426–4438, https://doi.org/10.1529/biophysj.108.132217.

[34] B.A. Aguado, W. Mulyasasmita, J. Su, K.J. Lampe, S.C. Heilshorn, Improving viability of stem cells during syringe needle flow through the design of hydrogel cell carriers, Tissue Eng. Part A 18 (2012) 806–815, https://doi.org/10.1089/ten.tea.2011.0391.

[35] R. Mckay, Stem cells in the central nervous system, Science (80-) 276 (1997) 66–71, https://doi.org/10.1126/science.276.5309.66.

[36] O.N. Suslov, V.G. Kukekov, T.N. Ignatova, D.A. Steindler, Neural stem cell heterogeneity demonstrated by molecular phenotyping of clonal neurospheres, Proc. Natl. Acad. Sci. U.S.A. 99 (2002) 14506–14511, https://doi.org/10.1073/pnas.212525299.

[37] Y. Elkabetz, G. Panagiotakos, G. Al Shamy, N.D. Socci, V. Tabar, L. Studer, Human ES cell-derived neural rosettes reveal a functionally distinct early neural stem cell stage, Genes Dev. 22 (2008) 152–165, https://doi.org/10.1101/gad.1616208.

[38] Y. Jin, A. Compaan, T. Bhattacharjee, Y. Huang, Granular gel support-enabled extrusion of three-dimensional alginate and cellular structures, Biofabrication 8 (2016) 25016, https://doi.org/10.1088/1758-5090/8/2/025016.

[39] K. Watanabe, M. Ueno, D. Kamiya, A. Nishiyama, M. Matsumura, T. Wataya, J.B. Takahashi, S. Nishikawa, S. Nishikawa, K. Muguruma, Y. Sasai, A ROCK inhibitor permits survival of dissociated human embryonic stem cells, Nat. Biotechnol. 25 (2007) 681–686, https://doi.org/10.1038/nbt1310.

[40] G.M. Ghobrial, K.D. Anderson, M. Dididze, J. Martinez-Barrizonte, G.H. Sunn, K. L. Gant, A.D. Levi, Human neural stem cell transplantation in chronic cervical spinal cord injury: functional outcomes at 12 months in a phase ii clinical trial, Clin. Neurosurg. (2017) 87–91, https://doi.org/10.1093/neuros/nyx242. Oxford University Press.